

The Disulfide Bond between Cys22 and Cys27 in the Protease Domain Modulate Clotting Activity of Coagulation Factor X

Fang Li^{1,*} Changming Chen^{2,*} Si-Ying Qu¹ Ming-Zhu Zhao³ Xiaoling Xie² Xi Wu² Lei Li²
Xuefeng Wang^{2,4} Qiulan Ding² Qin Xu¹ Dong-Qing Wei¹ Wenman Wu^{2,4,5}

¹ State Key Laboratory of Microbial Metabolism, School of Life Sciences and Biotechnology, Shanghai Jiao Tong University, Shanghai, China

² Department of Laboratory Medicine, Ruijin Hospital, Shanghai Jiao Tong University School of Medicine, Shanghai, China

³ Instrumental Analysis Center, Shanghai Jiao Tong University, Shanghai, China

⁴ Faculty of Laboratory Medicine, Shanghai Jiao Tong University School of Medicine, Shanghai, China

⁵ Collaborative Innovation Center of Hematology, Shanghai Jiao Tong University School of Medicine, Shanghai, China

Address for correspondence Qin Xu, PhD, 800 Dongchuan Road, Shanghai 200240, China (e-mail: xuqin523@sjtu.edu.cn).

Dong-Qing Wei, PhD, 800 Dongchuan Road, Shanghai 200240, China (e-mail: dqwei@sjtu.edu.cn).

Wenman Wu, MD, 197 Ruijin Second Road, Shanghai 200025, China (e-mail: wenmanwu@shsmu.edu.cn).

Thromb Haemost 2019;119:871–881.

Abstract

The Cys22-Cys27 disulfide bond of factor X (FX) protease domain is not conserved among coagulation factors and its contribution to the physiological haemostasis and implication in the pathogenesis of haemostatic and thrombotic disorders remain to be elucidated. Mutation p.Cys27Ser was identified in a pedigree of congenital FX deficiency and fluorescence labelling study of transiently transfected HEK293 cells showed accumulation of FX p.Cys27Ser within cell, indicating incompetent secretion partially responsible for the FX deficiency. The clotting activity of FX p.Cys27Ser was decreased to about 90% of wild-type, while amidolytic and pro-thrombinase activities (kcat/Km) determined with recombinant FXa mutant were 1.33- and 4.77-fold lower. Molecular dynamic simulations revealed no major change in global structure between FXa p.Cys27Ser and wild-type FXa; however, without the Cys22-Cys27 disulfide bond, the insertion of newly formed N terminal of catalytic domain after the activation cleavage is hindered, perturbing the conformation transition from zymogen to enzyme. The crystal structure of FXa shows that this disulfide bond is solvent accessible, indicating that its stability might be subject to the oxidation/reduction balance. As demonstrated with FX p.Cys27Ser here, Cys22-Cys27 disulfide bond may modulate FX clotting activity, with reduced FX pertaining less pro-coagulant activity.

Keywords

- ▶ coagulation factor X
- ▶ Cys27
- ▶ disulfide bond
- ▶ oxidation/reduction balance
- ▶ molecular dynamic simulations

Introduction

Coagulation factor X (FX) is the conjunction of intrinsic and extrinsic coagulation pathway. It activates pro-thrombin into

thrombin and is a key player in blood coagulation.¹ Decreased or elevated FX shifts the balance of haemostasis of blood and is associated with bleeding or thrombotic disorders. FX deficiency is a rare hereditary bleeding disorder, affecting 1 out of 1,000,000 general population, and is caused by genetic mutations of *F10* gene on chromosome 13.^{2,3} High-level FX in plasma, however, is a risk factor for venous thrombosis,

* Fang Li and Changming Chen equally contributed to this work.

Qin Xu's ORCID is <https://orcid.org/0000-0002-8346-9431>.

received

October 10, 2018

accepted after revision

January 30, 2019

© 2019 Georg Thieme Verlag KG
Stuttgart · New York

DOI <https://doi.org/>

10.1055/s-0039-1683442.

ISSN 0340-6245.

particularly when other vitamin K-dependent coagulation factors are within normal range.⁴ FX is a serine protease and shares high structural homology with other coagulation factors.⁵ The strictly conserved amino acid residues among different coagulation factors have been widely investigated because of their essential roles in the structure and function. The non-conserved amino acid residues, however, are not thoroughly studied, and their contribution to the integrity of structure and significance in coagulation functions of FX are not well understood. The amino acid residues Cys27 and Cys22 (nomenclature according to the chymotrypsin numbering system) of FX protease domain as well as the disulfide bond formed between them are only shared by coagulation FVII, but not found in other FX homology proteins, such as FIX, thrombin or protein C. With studies on patients with FX p.Cys27Ser mutations, in vitro expression and functional experiments, as well as molecular dynamics (MDs) simulations, we tried to elucidate the contribution of the disulfide bond between Cys27 and Cys22 to the synthesis and secretion of FX and probe its possible role in FX pro-coagulant activity regulation.

Materials and Methods

Patient and Pedigree

A 36-year-old female proband experienced menorrhagia since menarche and she had to receive plasma infusion to stop bleeding on some occasions. Her mother also complained about ecchymosis and heavy menstruation bleeding. The proband's father and son did not have obvious bleeding diathesis (► Fig. 1A).

Coagulation Function Assays

The peripheral blood was collected via venipuncture into tubes containing sodium citrate (final concentration 0.38%). Routine coagulation screening assays, including pro-thrombin time (PT), activated partial thromboplastin time (aPTT), fibrinogen (Fg), thrombin time, D-dimer and Fg/fibrin degradation products, were performed on an ACL-TOP automatic coagulometer (Instrumentation Laboratory, Bedford, Massachusetts, United States).

Plasma FX Activity and Antigen Determination

The FX clotting activity (FX:C) was measured using the aPTT and PT pathway-based coagulation function assays on the ACL-TOP automatic coagulometer (Instrumentation Laboratory). The plasma FX was activated to activated FX (FXa) by Russell's viper venom (RVV-X) (Haematologic Technologies Inc., Essex Junction, Vermont, United States) and its enzymatic activity was determined using specific chromogenic substrate S2765 (Hyphen-Biomed, Neuville-Sur-Oise, France). Antigen level of FX (FX:Ag) was measured using an enzyme-linked immunosorbent assay (ELISA) kit (Enzyme Research Laboratories, South Bend, United States).

Genetic Analysis of F10

Genomic deoxyribonucleic acid (DNA) was extracted from peripheral whole blood using the QIAamp DNA blood purification kit (Qiagen, Hilden, Germany). The coding sequences and flank regions of F10 gene were amplified by polymerase chain reaction and sequenced thereafter. The primers used are listed in ► Supplementary Data (► Table S1, available in the online version).

In Vitro Recombinant FX Expression and Coagulation Activity Characterization

The plasmid containing FX p.Cys27Ser variant encoding sequence was constructed by site-directed mutagenesis (Agilent Technologies Inc., Santa Clara, California, United States), and transfected into HEK-293 cells with Lipofectamine 2000 (Invitrogen, Carlsbad, California, United States). The transfected cells were maintained in Dulbecco's Modified Eagle Medium/F12 medium supplemented with 10 µg/mL vitamin K1 for 24 hours. The expressed FX p.Cys27Ser mutant was isolated from supernatants of conditioned culture medium by ion exchange chromatography using HiTrap SP ion exchange column (GE Healthcare Life-Science, Uppsala, Sweden). Approximately 0.4 M CaCl₂ containing Tris-buffered saline (TBS) buffer (0.02 M Tris-HCl, 0.1 M NaCl, pH 7.4) was applied to elute fully γ-carboxylated FX protein from the ion exchange column. The isolated recombinant FX protein was subjected to sodium dodecyl sulphate-polyacrylamide gel electrophoresis

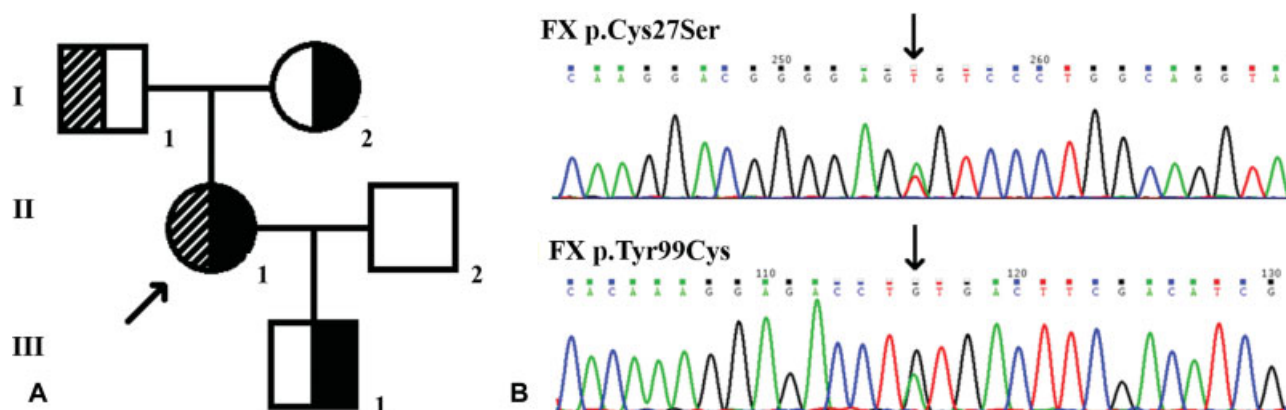


Fig. 1 The phenotypic and genetic analysis of proband and pedigree. (A) Two F10 genetic variances were identified in the probands, c.736t > a and c.956a > g, which led to amino acid replacements p.Cys27Ser and p.Tyr99Cys. (B) The pedigree analysis traced the two mutations of the proband (II-1) back to both parents, respectively, with the p.Cys27Ser from father (I-1) and p.Tyr99Cys (I-2) from mother, which was also passed onto the proband's son (III-1).

on a 10% polyacrylamide gel under non-reducing conditions to examine the homogeneity and purity of the isolated wild-type (WT) and mutant FX derivatives. The concentration of purified recombinant FX protein was determined by ELISA as described previously. The clotting activity of recombinant FX and its variant were determined using aPTT- and PT-based coagulation function tests following similar protocol mentioned above.

Determination of the FX Activation by the FVIIa–Tissue Factor Complex

The initial rate of activation of both recombinant wide-type and mutant FX (0–400 nM) by FVIIa (0.1 nM) in complex with tissue factor (TF) (2 nM) was monitored on phosphatidylcholine/phosphatidylserine (PC/PS) vesicles in TBS/Ca²⁺ for 3.5 minutes at room temperature in 30 µL reactions as described.⁶ Activation reactions were terminated by addition of 30 µL of ethylenediaminetetraacetic acid (EDTA) and subjected to amidolytic assay using S2765 as substrates. The concentration of FXa generated was determined by comparing its S2765 hydrolytic activity against standard curves prepared by serial diluted FXa (0–200 nM).

The Kinetic Analysis of FXa Amidolytic Activity

The amidolytic activity of FXa was characterized with steady-state kinetics analysis of hydrolysis of chromogenic substrates S2765. The FXa derivatives (2 nM) was incubated with various concentration of S2765 (25–1,600 µM) in TBS/Ca²⁺ buffer (0.02 M Tris-HCl, 0.1 M NaCl, 0.1 mg/mL bovine serum albumin, 0.1% polyethylene glycol 8000 and 5 mM Ca²⁺, pH 7.4) at room temperature for 15 minutes on a microplate reader (Molecular Devices, Menlo Park, California, United States). The rate of hydrolysis was recorded at 405 nm and the Km and kcat values were calculated with the Michaelis–Menten equation and the specificity of WT and mutant FX was determined using the ratio of kcat/Km.

Determination of the Activation of Pro-Thrombin by FXa

The concentration dependence of pro-thrombin activation by FXa derivatives was determined in the absence and presence of FVa on PC/PS vesicles as described.⁷ Briefly, in the absence of FVa, pro-thrombin (0–2 µM) was incubated with each FXa (10 nM) in TBS/Ca²⁺ on PC/PS vesicles (25 µM) at room temperature for 30 to 90 minutes. EDTA was added to a final concentration of 20 mM and the initial rate of pro-thrombin activation was monitored from the rate of thrombin generation detected by an amidolytic activity assay using 450 µM S2238. The standard curve was prepared from the cleavage rate of S2238 by known concentrations of recombinant thrombin under the same conditions. In the presence of human FVa (20 nM), increasing concentration of pro-thrombin (30–2,000 nM) was incubated with each FXa derivative (0.1 nM) in TBS/Ca²⁺ on PC/PS vesicles (25 µM) for 1.5 minutes at room temperature. After the termination by EDTA, the concentrations of thrombin generated were determined from a standard curve as described above. Kinetic constants Km(app) and kcat were calculated from the Michaelis–Menten equation.

Determination of Binding Affinity of FVa and FXa

The binding affinity of FVa and FXa was determined using similar pro-thrombinase assay described above. The pro-thrombin activation by both WT and mutant FXa in the presence of various FVa concentrations was measured. The pro-thrombin (1 µM) was incubated with FXa (WT or mutant) (50 pM) and increasing concentration of FVa (0–5 nM) on PC/PS vesicles (25 µM) for 30 seconds. The rate of thrombin generation was determined as described above.

Immunofluorescence Analysis of FX Expression and Secretion

HEK 293 cells were seeded on polylysine pre-treated coverslips placed in 6-well cell culture plates. After transient transfection of wide-type FX or C27S-mutate FX, coverslips were fixed in 4% formaldehyde. The intra-cell FX molecules were detected by sheep anti-human FX antibody (Haematologic Technologies Inc.). The endoplasmic reticulum (ER) and Golgi were stained using Mouse anti-GM130 and SERCA2 ATPase Antibody Monoclonal (IID8) (Thermo Fisher, Waltham, Massachusetts, United States). Donkey anti-mouse immunoglobulin G (H + L)-Alexa Fluor 568 and mouse anti-sheep fluorescein isothiocyanate (Thermo Fisher) were used as secondary antibodies. The nucleus was stained with 4',6-diamidino-2-phenylindole (Thermo Fisher). The fluorescence signal was visualized with confocal microscope (Leica TCS SP8 MP, Solms, Germany).

Molecular Dynamics Simulations

Based on the X-ray structure of the activated FXa (PDB ID: 2W26),⁸ a molecular model was constructed for the WT FXa, which then had the Cys22-Cys27 disulfide bond locally broken into two thiols called disulfide broken (DISB) WT, or had Cys27 mutated into serine (MT), respectively. Only the heavy chains of FXa were included in the models to simulate the structures after the cleavage. The N-terminal segments (residues 16–22) of these models were also remodelled by Modeller module of Chimera⁹ in a possible extended conformation just after the cleavage. All the models above were solvated in a periodic cubic water box with a buffer distance of 10 Å between the protein and the box edges, where the explicit water molecules were described by the TIP3P model. To obtain an electrically neutral system, the GENION tool from the GROMACS package was used to randomly replace water molecules with the appropriate number of counter ions Cl⁻. The six MD simulation systems are summarized in **►Supplementary Table S2** (available in the online version). Using GROMACS 5.1.2 with the CHARMM36 force field, the systems were energy-minimized with the steepest descent method to a convergence on the maximal force of 100 kJ/mol/nm, followed by a short 100 ps NVT simulation at 310 K and then a 100 ps NPT MD simulation at 310 K and 1 atm.^{10,11} Then, further NPT MD simulations were performed for more than 300 ns under the same condition. With the LINCS algorithm applied to the lengths of hydrogen involved bonds, the time step of the simulations was set to 2 fs.¹² And the coordinates were saved at a regular interval of 10 ps. Structural properties such as the root-mean-square deviation, the root-mean-square fluctuation (RMSF), clusters and distances between Ile16 and Asp194 were calculated with

GROMACS standard analysis tools and visual MD.¹³ Considering possible rotation of the carboxyl group of Asp194, here the distance between Ile16 and Asp194 was simply defined as the atomic distance between Ile16N_ζ and Asp194C_γ.

Results

Patient Data

Although the plasma FX:Ag of the proband only mildly decreased (69.7% of normal control), the clotting time was prolonged in both the aPTT and PT tests. The FX:C determined by all three means, including aPTT-, PT- and RVV-based methods, was consistently around 20% of normal of control. However, the amidolytic activity as determined by chromogenic assay using S2765 was only mildly compromised (around 68.3% of normal control). The coagulation function analysis of other family members showed that both aPTT and PT were within normal reference range (►Table 1), but all of them had their FX:C partially decreased. The FX:C of proband's father (I-1) was around 75% of normal, which was consistent

with his antigen level as well as chromogenic activity; the patient's mother (I-2) and son (III-1) had almost normal FX:Ag and chromogenic activity; however, their FX:C decreased to lower borderline of the reference range (~50% of normal control). Genetic analysis of proband's *F10* gene revealed two single nucleotide changes, c.736t > a and c.956a > g, which predicted missense mutations p.Cys27Ser and p.Tyr99Cys (►Fig. 1B). The proband inherited p.Tyr99Cys from her mother (I-2) and had it passed onto her son (III-1). The discrepancy of FX:Ag and FX:C of both p.Tyr99Cys mutation carrier suggested that the mutant was a cross-reactive material positive mutation (CRM+) and the deficiency was mainly caused by impaired function of FX mutant. The other mutation p.Cys27Ser was traced back to proband's father (I-1) and its impact on function and expression of FX warranted further study to characterize (►Table 1).

Coagulation Activity of Recombinant FX Mutant

The recombinant WT FX and FX p.Cys27Ser mutant showed similar migrant pattern on Western blot (►Fig. 2A). The

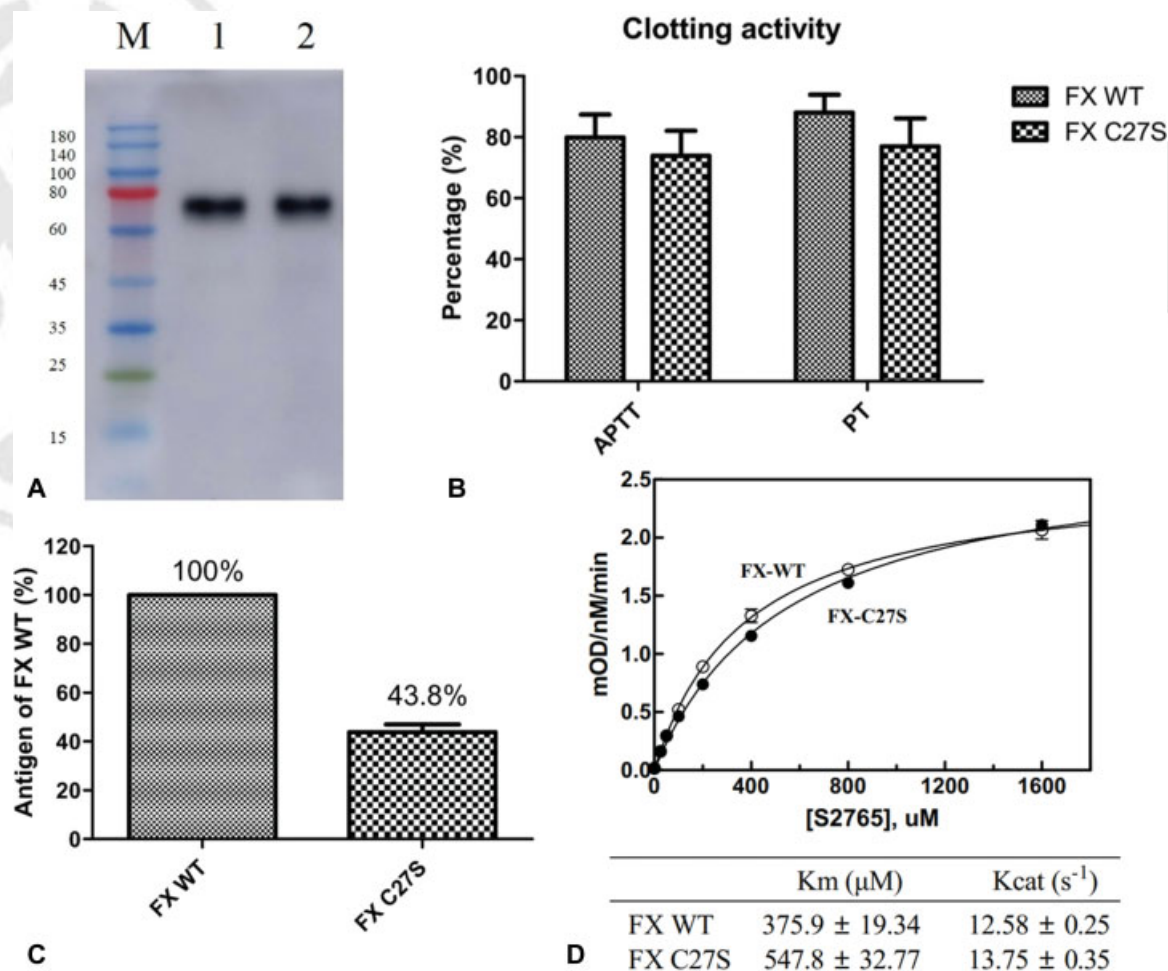


Fig. 2 In vitro expression and characterization of factor X (FX) mutant. (A) The migration pattern of recombinant FX mutant p.Cys27Ser is similar to that of the wild-type FX. (B) The clotting activity of FX mutant p.Cys27Ser, as determined by both pro-thrombin time (PT)- and activated partial thromboplastin time (aPTT)-based clotting assays, is mildly decreased to around 90% of wild-type FX. (C) The transient expression of FX in HEK293 cells yields less FX p.Cys27Ser mutant in conditioned medium, about 43.8% of wild-type FX. (D) The impact of Cys27Ser mutation on enzymatic activity of FX was determined by amidolytic assays using chromogenic substrate S2765. Comparing with wild-type FXa, the K_m of activated FX p.Cys27Ser mutant towards substrate moderately increased (375.9 ± 19.34 μM vs. 547.8 ± 32.77 μM); however, its k_{cat} was similar to that of wild-type FXa (12.58 ± 0.25 s⁻¹ vs. 13.75 ± 0.35 s⁻¹).

clotting activity of FX mutant p.Cys27Ser determined by PT- and aPTT-based clotting assays mildly decreased to around 90% of WT FX (►Fig. 2B). The FX mutant p.Cys27Ser collected from supernatant of conditioned medium was much less than WT (43.8%), suggesting possible impediment of synthesis or secretion of the mutant (►Fig. 2C).

Kinetic Analysis of FX p.Cys27Ser Cleavage of Chromogenic Substrate

The amino acid replacement increased the K_m from 375 to 547 μM , but had little effect on the k_{cat} (12.58 vs. 13.75 s^{-1}) (►Fig. 2D), suggesting the cleavage of chromogenic substrate S2765 by FX p.Cys27Ser was only marginally affected (1.33-fold change of k_{cat}/K_m).

FX Activation by FVIIa–TF Complex

The activation of FX by its physiological activator FVIIa–TF complex was slowed by the amino acid substitution p.Cys27Ser, with a 1.57-fold higher K_m (from 90.44 to 142.4

nM) and 2.17-fold lower k_{cat} (from 325.6 to 149.9 min^{-1}) (►Fig. 3A).

Activation of Pro-Thrombin by FXa and Pro-Thrombinase Complex

Similar to the amidolytic assay, the pro-thrombin activation activity by FX p.Cys27Ser mutant was impaired significantly, with a much smaller k_{cat} (1.39 vs. 10.83 min^{-1} of WT FXa) and greater K_m (1031.0 vs. 365.2 nM of WT) (►Fig. 3C). Interestingly, the difference between WT and p.Cys27Ser mutant became minimal when FVa was present. The k_{cat} of WT FXa and mutant was both increased dramatically (1,139 vs. 1,221 min^{-1}), and K_m decreased to 139.5 and 713.6 nM, yielding 4.77-fold change of k_{cat}/K_m between WT FXa and mutant (8.16 vs. 1.71) (►Fig. 3D; ►Table 2).

Binding Affinity of FXa Mutant p.Cys27Ser and FVa

The binding between FVa and FX was not affected significantly by the mutation p.Cys27Ser. The K_d determined was

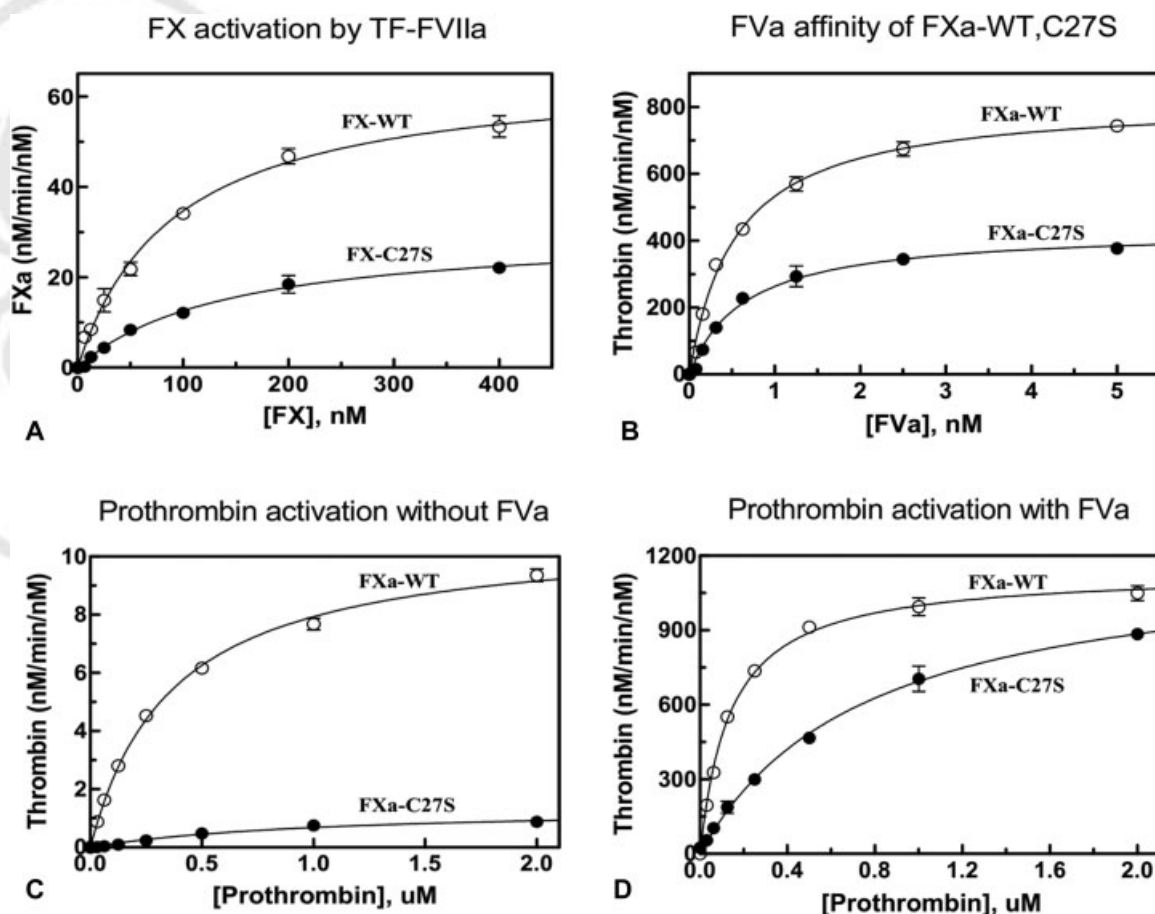


Fig. 3 The kinetic analysis of factor X (FX) activation by FVIIa–tissue factor (TF) and pro-thrombinase activity determination. (A) FX-wild-type (WT) (○) or FX-C27S (●) were activated by FVIIa (0.1 nM) in complex with TF (2 nM) on phosphatidylcholine/phosphatidylserine (PC/PS) vesicles in Tris-buffered saline (TBS)/ Ca^{2+} for 3.5 minutes at room temperature. The reactions were terminated by 20 mM ethylenediaminetetraacetic acid (EDTA) and the FXa generation was determined from standard curves as described in the ‘Materials and Method’ section. (B) The activation of pro-thrombin (1 μM) by FXa-WT (○) and FXa-C27S (●) (50 pM) was monitored in the presence of different concentrations of FVa (0–5 nM) on PC/PS vesicles (25 μM) in TBS/ Ca^{2+} for 30 seconds. Note that 20 mM EDTA was added to terminate reaction and the rate of thrombin generation was measured as described in the ‘Materials and Method’ section. (C) In the absence of FVa, various concentrations of pro-thrombin (0~2 μM) were incubated with 10 nM of either FXa-WT (○) or FXa-C27S (●) on PC/PS vesicles in TBS/ Ca^{2+} . Following 30 to 90 minutes’ incubation, EDTA was added to a final concentration of 20 mM and the initial rate of thrombin generation was measured from the cleavage rate of S2238 as described in the ‘Materials and Method’ section. (D) It is the same as (C) except that the activation reactions by each FXa derivatives (0.1 nM) were carried out in the presence of FVa (20 nM) for 1.5 minutes.

Table 1 The clotting function and genetic profile of the pedigree

	aPTT (s)	PT (s)	FX:C (%) – Clotting activity			FX:C (%) – Chromogenic activity	FX:Ag (%)	F10 mutation
			aPTT	PT	RVV			
Proband	48.3	20.2	22.1	20.0	22.3	68.3	69.7	Cys27Ser/Tyr99Cys
I-1	37.4	13.8	69.8	75.2	75.8	70.0	73.0	Cys27Ser (Het)
I-2	35.0	14.6	53.5	50.6	53.5	95.3	92.5	Tyr99Cys (Het)
III-1	27.8	11.5	50.9	49.8	53.3	90.6	102.4	Tyr99Cys (Het)
Reference	27.2–41.0	10.0–16.0	50–150	50–150	50–150	50–150	50–150	

Abbreviations: aPTT, activated partial thromboplastin time; FX, factor X; PT, pro-thrombin time; RVV, Russell viper venom.

Table 2 Kinetics of pro-thrombin activation by FXa derivatives and the apparent dissociation constants Kd(app) for their interaction with FVa

	Km(app) (nM)	kcat (min ⁻¹)	kcat/Km (nM/min)	FVa, Kd(app) (nM)
FXa-WT				
Pro-thrombin, PC/PS, Ca ²⁺	365.2 ± 20.58	10.83 ± 1.056	29.65*10 ⁻³	
Pro-thrombin, PC/PS, Ca ²⁺ , FVa	139.5 ± 7.97	1,139 ± 88.1	8.16	0.545 ± 0.037
FXa-C27S				
Pro-thrombin, PC/PS, Ca ²⁺	1031.0 ± 173.90	1.39 ± 0.314	1.35*10 ⁻³	
Pro-thrombin, PC/PS, Ca ²⁺ , FVa	713.6 ± 93.24	1,221 ± 240.6	1.71	0.652 ± 0.078

Abbreviations: FXa, factor Xa; PC, phosphatidylcholine; PS, phosphatidylserine; WT, wild-type.

Note: The kinetics constants Km(app) and kcat were determined from the concentration dependence of pro-thrombin activation by FXa derivatives as described in the 'Materials and Method' section. The Kd(app) values for the interaction of each FXa derivatives with FVa were determined by the same assay with various concentration of co-factor. The data are representative of two to three independent measurements.

0.545 nM for WT FXa and 0.652 nM for FXa p.Cys27Ser mutant (► Fig. 3B).

Immunofluorescence Staining of FX Derivatives in Transiently Transfected Cells

The immunofluorescence staining of FX (► Fig. 4A and C) or FX mutant (► Fig. 4B and D) intra-transiently transfected HEK-293 cell showed dramatically increased retention of FX molecule. Most of the recombinantly expressed FX Cys27Ser accumulated within the ER system (► Fig. 4B), and to a less extent, in the Golgi body (► Fig. 4D), which might be responsible for inefficient secretion of FX Cys27Ser mutant as observed previously. The fluorescence intensity of FX Cys27Ser mutant was 1.5-fold higher than WT (► Fig. 4E).

Molecular Dynamics Simulations of Cleaved FXa Models in the Activated Conformation

Based on the X-ray structure of the activated FXa (PDB ID: 2W26), molecular models were constructed for the WT, Cys27Ser mutant (MT) and a WT FXa with the Cys22-Cys27 DISB WT, as shown in ► Supplementary Table S2 (available in the online version). Starting from the initial models, all systems were simulated for more than 300 ns. After about 60 ns simulations, all the systems tended to be equilibrated. In this activated conformation, all the three systems have the N-terminal inserted into the activation pocket all the time, with Ile16 relatively fixed to Asp194 by a salt bridge (► Fig. 5). Comparison between the three systems

showed almost no difference in the fluctuations at the N-terminal segment (► Fig. 5A), variations in the distance between Ile16 and Asp194 (► Fig. 5B) or the local positions of the critical residues Ile16, Asp194 and Ser195 in the activation pocket and the catalytic pocket (► Fig. 6). The hydrogen bonds network around the activation pocket and the backbone hydrogen bonds between Gln20 and Met156 to form an untypical β sheet are also observed. These results suggested that the structure of the catalytic site of the activated FXa might not be changed importantly in the Cys27Ser mutant. Also, considering that the relative position of the mutation site is far from the catalytic site, it is highly possible that the amino acid substitution does not change the amidolytic activity of FXa directly. Instead, it might hinder the early phase of conformation switch from inactive zymogen (FX) to enzyme with hydrolytic activity (FXa) after the scissile bond between heavy chain and light chain is cleaved, that is, the insertion of the N-terminal from the just cleaved position into the activation pocket.

Simulations of the Insertion of the N-Terminal into the Activation Pocket

In order to construct the models prior to the insertion, the N-terminal segments (residues 16–22) of the systems above were remodelled by Modeller in a possible extended conformation after the cleavage activation. In simulations of these systems, the N-terminal of the cleavage site was initially swinging around far from the activation pocket. Possibly because of

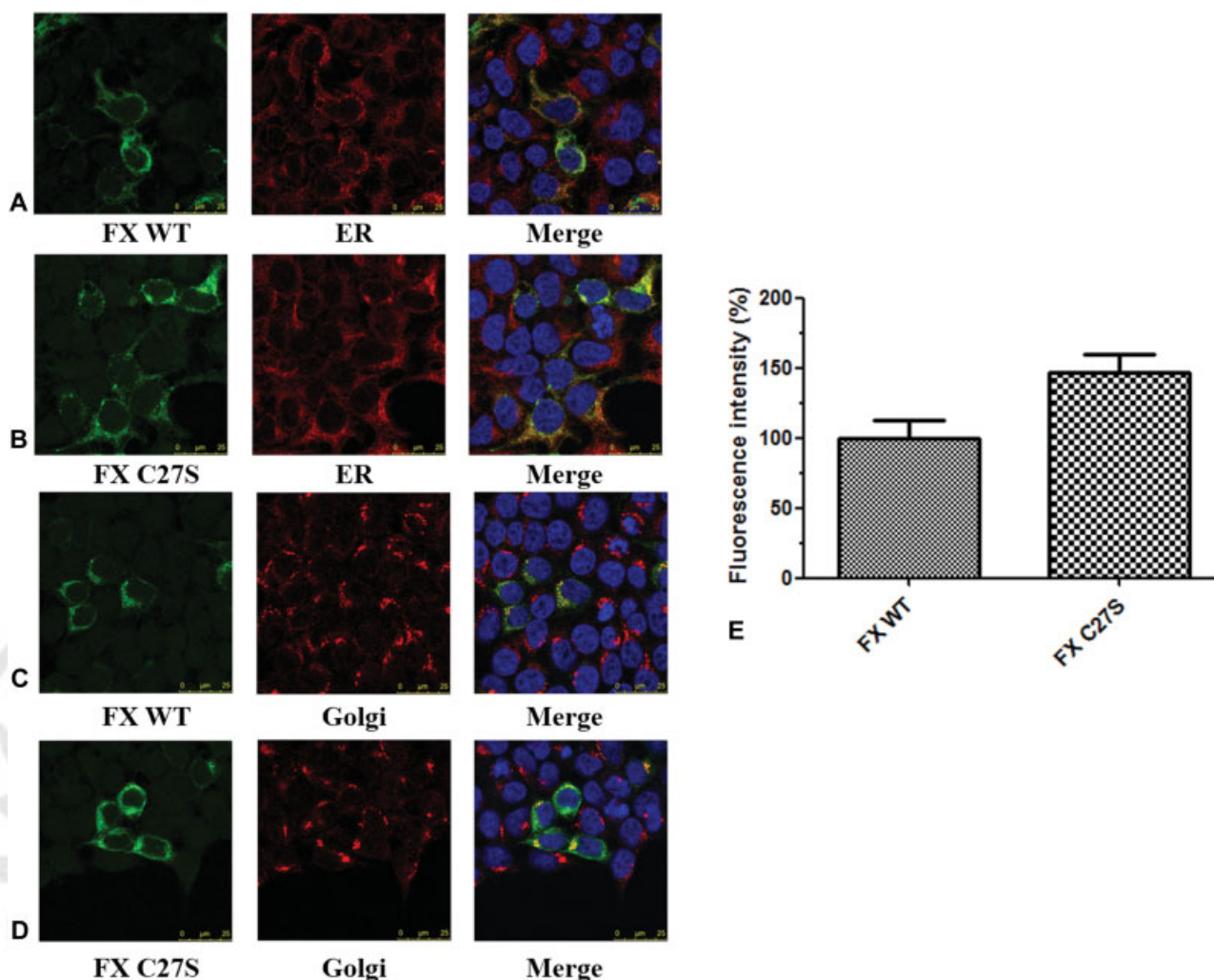


Fig. 4 The immunofluorescence staining of factor X (FX) derivatives in transiently transfected cells. The expression and secretion of FX Cys27Ser. The HEK 293 cells were transiently transfected with wild-type FX and FX Cys27Ser mutation expressing plasmid. The synthesis and secretion of FX were traced with fluorescence-labelled FX-specific antibodies (red), the cell nucleus were stained with 4',6-diamidino-2-phenylindole (DAPI) (blue). The Golgi body and ER were also stained (red) to locate FX. (A) FX wild-type (WT) (green) + ER (red) + Merged; (B) FX Cys27Ser + ER + Merged; (C) FX WT + Golgi + Merged; and (D) FX Cys27Ser + Golgi + Merged. (E) The accumulation of synthesized FX and FX Cys27Ser mutant within cells was estimated by fluorescence intensity measurement.

the tethering of the Cys22-Cys27 disulfide bond, the swing in the WT system was relatively limited and the N-terminal segment was quickly anchored to the edge of the activation pocket, formed two strong backbone hydrogen bonds between Gln20 and Met157, which somewhat integrated the N-terminal segment into the core β sheet. This anchoring greatly further limited the fluctuation of the N-terminal segment. Although the end (Ile16 to Gly19) still wandered at the entry of the pocket for a period, it gradually entered into the activation pocket and formed the Ile16-Asp194 salt bridge spontaneously after 150 ns. On the other hand, the mutant and the WT systems with Cys22-Cys27 DISB both had the N-terminal segment wander around far away outside the pocket in the 300-ns simulations, meaning the insertion is importantly delayed (\rightarrow Fig. 7). Correspondingly, RMSF analyses showed more and more fluctuations in the length of the N-terminal segment and in the extent of fluctuations in the WT, DISB WT and MT systems, respectively (\rightarrow Fig. 5A). This difference is also obvious in comparison of the Ile16-Asp194 distances in

\rightarrow Fig. 5B. After a short time of equilibration, the WT enzyme (in cyan) had the distance gradually shortened from 2 to 0.3 nm, which is consistent to a salt bridge; the DISB WT (in magenta) stayed nearly 2 nm; the mutant (in orange) stayed at 2 nm for about 200 ns and, after that, the N-terminal moved away back to about 3 nm. And clustering analyses also found more concentrated distribution in the WT system around the inserted conformation versus much more scattered distribution in the mutant (\rightarrow Supplementary Figs. S2 and S3, available in the online version).

Discussion

The coagulation FX is a serine protease zymogen, belonging to the trypsin family just like other components of the coagulation cascade. Evolved by gene duplications from the same ancestry, FX has high homology with other coagulation factors, such as FIX, FVII, FXI and pro-thrombin.¹⁴ The strictly conserved residues shared among the coagulation factors are

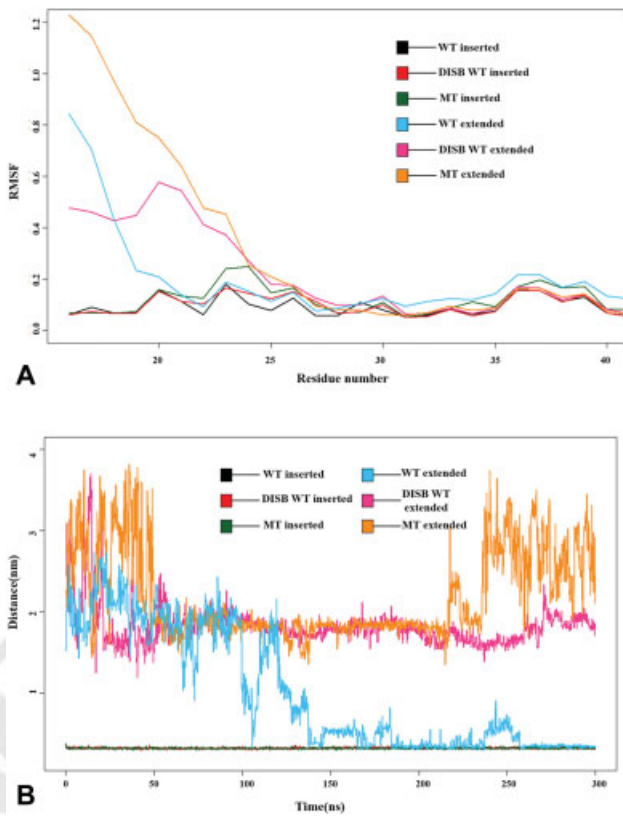


Fig. 5 Fluctuations of the N-terminal segments. (A) The root-mean-square fluctuations (RMSFs) of the N-terminal residues 16 to 51, showing the fluctuations of their backbone atoms. (B) Distances between the side chains of Ile16 to Asp194, which was defined as the atomic distance of Ile16N ζ to Asp194C γ .

critical to the structure and function integrity,¹⁵ and mutations involving these sites lead either to null expression or complete loss of function.^{16–19} The non-conserved residues constitute significant portion of FX sequence; however, their significance in structure and function have not been fully revealed.

Naturally, FX exists as a mixture of molecules in zymogen or enzyme conformations.²⁰ Before cleavage and activation, the zymogen conformation is preferred. And once the scissile peptide bond between the heavy and the light chains is cleaved, the balance shift to the activated enzyme decisively. As other serine protease homologous to trypsin, this cleavage forms a new N-terminal of the catalytic domain, whose first eight amino acid residues take a dramatic movement and insert into the activation pocket around Asp194.²¹ Camire and colleagues showed that mutations at the N-terminal of the FX catalytic domain will maintain zymogenicity of FX and become resistant to its inhibitors.²² In the X-ray structure of FXa (PDB ID: 2W26), Asp194 and Ile16 form a featured strong salt bridge in the activation pocket. In the meanwhile, the activated conformation may be further stabilized by a network of hydrogen bonds around the pocket, such as between Asp194 carboxyl and backbone of Gly142 and Cys191, the amino group of Ile16 and backbone of Arg143, the amino group of Lys156 and backbone of Ile16 and Gly18 and the backbone of Val17 and Asp189. In addition, at the edge of the

activation pocket, the backbone hydrogen bonds between Gln20 and Met157 can form an untypical β sheet, which is also observed in other coagulation factors like FII, FVII, FIX and FXI.^{23–26} These interactions provide an extra anchor to fix the N-terminal segment at the entry of the activation pocket and facilitate the insertion. At last, Cys22 lies at the root of the swing N-terminal segment and forms a disulfide bond with Cys27. However, both the two cysteine residues and the disulfide bond between them are not totally conserved among the coagulation factors of the serine protease family. The contribution of the Cys22-Cys27 disulfide bond to the conformational transition of FX activation and enzymatic activity of FXa is still not clear. It is interesting to explore the effect of this disulfide bond on the enzyme conformation and its implication to the enzyme function.

The naturally occurring mutation p.Cys27Ser of FX provides important clues to the residues' contribution in physiological haemostasis and pathological thrombosis. *F10* gene mutations either lead to insufficient expression or secretion of FX or encode FX with defective clotting activity. The FX deficiency is thus grossly sub-divided into two categories, CRM+ and CRM negative (CRM-), according to the ratio between residual FX:C and FX:Ag.²⁷ The p.Cys27Ser mutation was identified in patients with compound *F10* mutations and the genotypic and phenotypic study of the patient and pedigree members showed that the mechanism underlying FX deficiency caused by mutation p.Cys27Ser cannot be attributed to either category exclusively. Both FX:Ag and FX:C decreased in heterozygous carrier of mutation p.Cys27Ser; however, unlike typical CRM- mutations, the FX:Ag and FX:C level are not consistent, with reduction of FXI:C more prominent than FXI:Ag. The in vitro expression study showed similar effect of mutation p.Cys27Ser on FX:C and FX:Ag, suggesting that amino acid substitution p.Cys27Ser not only impairs the expression and secretion of FX, but also compromises the zymogen activation or enzyme activity of FX.

The p.Cys27Ser replacement disrupts the disulfide bond, and as the results of most amino acid replacement, unorthodoxically folded FX mutant is thus accumulated in the ER system, leading to decreased FX:Ag in circulation. The FX p.Cys27Ser mutant, which passed quality control in the ER system and secreted into circulation, cannot be converted into its active form as efficient as its WT counterpart; furthermore, the enzymatic activity of activated FXa p.Cys27Ser mutant also becomes lower than WT FXa. The enzymatic kinetic analysis revealed higher K_m and almost unaltered k_{cat} towards synthetic chromogenic substrate, suggesting reduced binding affinity between the FXa enzyme and substrate. It is also interesting to note that although the impairment of FXa enzymatic activity by amino acid substitution p.Cys27Ser against its physiological substrate, pro-thrombin, is dramatic, the functional defect of the pro-thrombinase complex is relatively minor, which may attribute to the conformational change facilitated by co-factor FVa.²²

In order to explore the molecular mechanism of the differences between WT FX and FX mutant p.Cys27Ser, we compared the conformations and the dynamic motions of the Cys27Ser mutant and the WT FXa with the Cys22-Cys27 disulfide bond formed and broken, especially around the

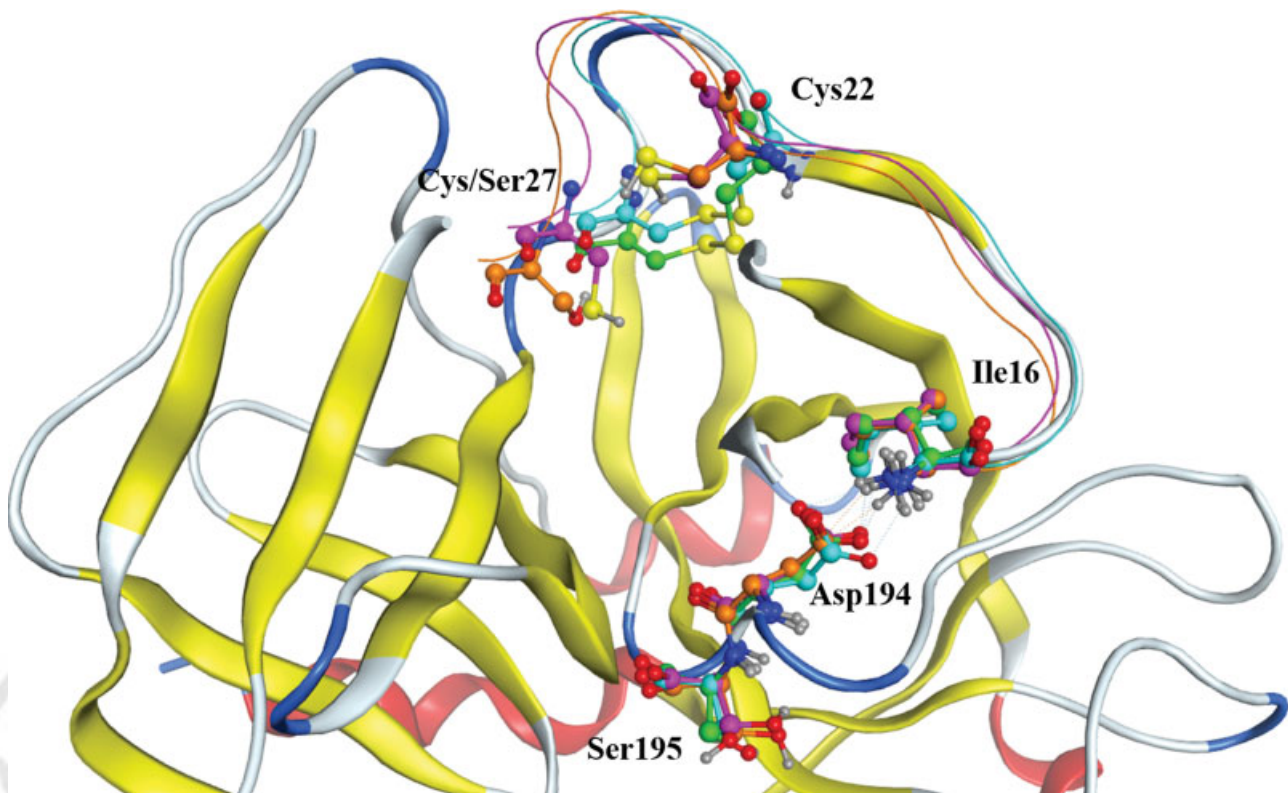


Fig. 6 Comparison of the activated conformations. The critical residues at the mutation site (Cys22 and Cys/Ser27), the activation pocket (Ile16, Asp194) and the catalytic site (Ser195) are visualized. Their oxygen atoms are coloured in red, nitrogen in blue, sulphur in yellow, hydrogen in grey, as well as their carbon atoms are coloured in cyan, magenta, orange and green for the wild-type (WT), disulfide broken (DISB) WT, mutated into serine (MT) systems and the template 2W26. The backbones of the N-terminal segment 16 to 27 of the three models (thin lines in cyan, magenta and orange in the same order) are also compared with the template 2W26, whose whole backbone are shown in cartoon and coloured by secondary structure, except that the loops of 70 to 79 and 142 to 153 are hidden for clarity.

activation pocket, by MD simulations.¹⁸ With an advantage in microscopic details, MD simulations have long been applied to studies on the molecular mechanism and drug design of FX coagulation factor, together with crystallographic analyses.^{28,29} However, most of those studies focused on the catalytic pocket or the specificity site, as far as we know, for the first time the activation pocket around Asp194 is looked as the target of MD simulations in this study. According to our MDs simulations, similar stable structures and interaction patterns were found in the inserted conformation of all the three systems, which may suggest similar final active form of these enzymes that resulted in similar k_{cat} of WT and the Cys27Ser mutant. At the same time, the N-terminal segment in the conformation prior to the insertion is quite different. In the WT FXa with Cys22-Cys27 disulfide bond, the fluctuation of the N-terminal segment is quite limited and would be more easily transitioned into the inserted conformation. On the other hand, if the disulfide bond is broken by reduction or by Cys27Ser mutation, the N-terminal segment had higher possibility to overhang outside the activation pocket with great fluctuations. This difference in efficiency of insertion may partially contribute to the slower conversion of FX p. Cys27Ser zymogen to its active enzyme form. The hindrance of newly formed N-terminal insertion may also suggest higher portion of FX p.Cys27Ser mutant still maintain its

zymogen conformation even after the cleavage of the scissile bond between heavy chain and light chain, which might lead to lower binding affinity, that is, the higher K_m of the mutant FXa with its substrates than the WT.

It should be noted that the Cys22-Cys27 disulfide bond is solvent accessible and its formation and disruption might be subjected to the influence of the oxidation/reduction balance in plasma. Therefore, the equilibration of the two species of FX, with or without the disulfide bond, could potentially shift, depending on the environmental oxidization pressures in the circulation. It has been shown that the formation and reduction of solvent accessible disulfide bond may work as a redox switch to regulate protein function. The intra-chain disulfide bond of Cys6-Cys11 of recombinant insulin was reported to affect the chain flexibility.³⁰ It has also been shown that the disulfide bond formation and disruption regulate the angiotensin release.³¹ The transition of angiotensinogen under oxidative environment to its more active form with sulphhydryl-bridged plays an important role in pregnancy hypertension and pre-eclampsia. As shown in this study, the FX molecules with the Cys22-Cys27 disulfide bond is functionally advantageous over FX with the disulfide bond reduced. It has been shown that the oxidation pressure is significantly related to the thrombus formation. The simple oxidation/redox balance shift could significantly disturb coagulation reaction in vitro. The FX with Cys22-Cys27

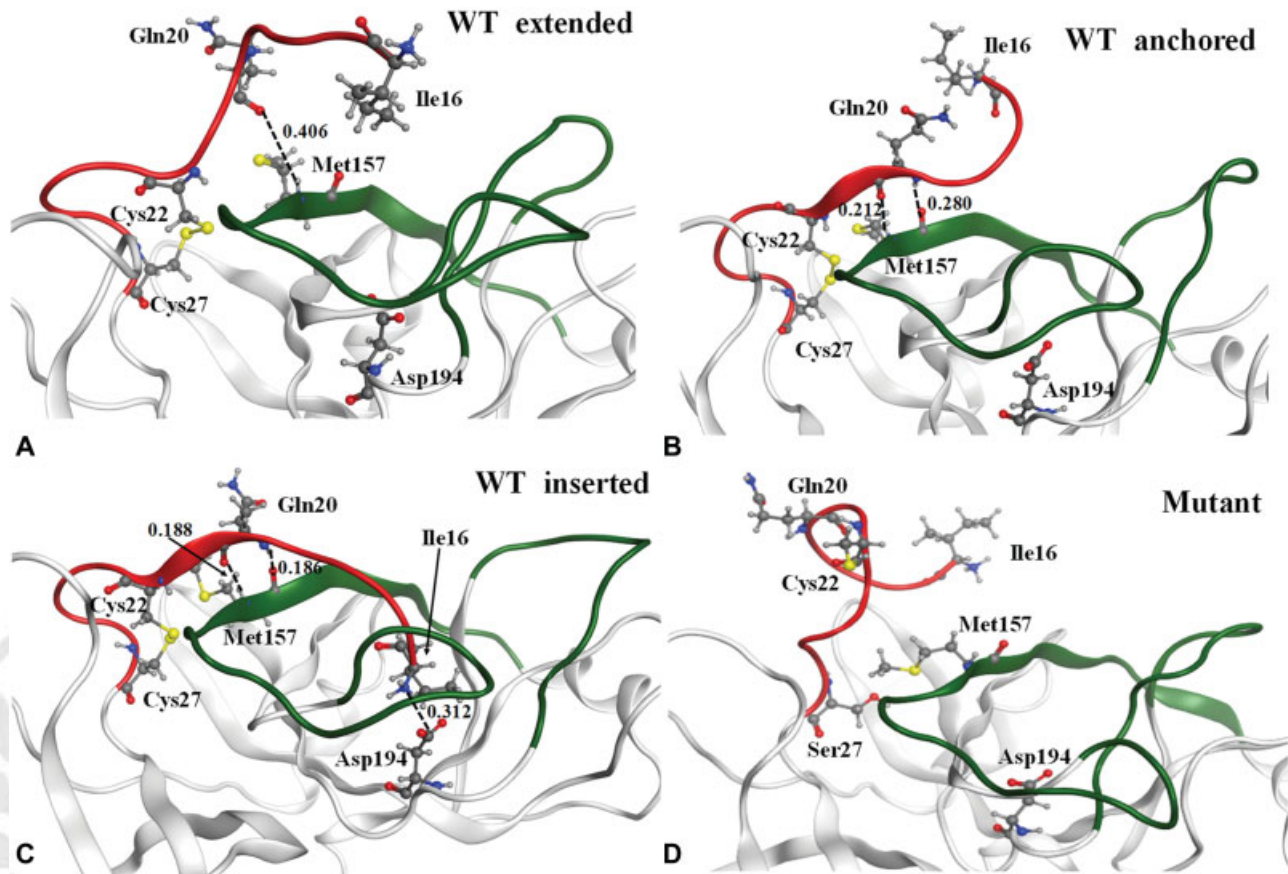


Fig. 7 Simulations of the just cleaved models of the wild-type (WT) and the mutant factor Xa (FXa). (A–C) The N-terminal segment of WT is spontaneously inserted into the activation pocket from the initially extended conformation (A), via an intermediate anchored conformation (B) and finally to the inserted conformation (C). On the other hand, the N-terminal segment of the mutated into serine (MT) system stays at the extended conformation (D) and swings around within the 300-ns simulation.

disulfide bond could be a more prominent form in milieu of vascular injury due to similar oxidation pressure and promote coagulation reactions and may thus contribute to the pathogenesis of thrombus upon atherosclerotic lesions.

Future investigations are warranted to explore the relationship between Cys22-Cys27 disulfide bond and oxidation/redox balance in plasma and its implication in pathogenesis of thrombosis.

What is known about this topic?

- The conversion of coagulation factor X to its active form factor Xa upon cleavage between heavy and light chains is triggered by insertion of newly formed N terminal of catalytic domain into preformed “activation pocket.”

What does this paper add?

- The disruption of non-conserved disulfide bond Cys22-Cys27 by mutation p.Cys27Ser not only hinders secretion of factor X, but also perturbs zymogen to enzyme conformation transition and impairs catalytic activity of factor Xa.

Authors' Contributions

F.L. performed molecular dynamic simulations and analysis; C.C. performed protein expression collection and purification and enzyme kinetical analysis; S.Q. and M.Z. contributed to discussion and manuscript revision of MD results; X.W. performed clinical data acquisition; X. X. and L.L. performed phenotype and genetic analysis; X. W. and Q.D. supervised studies conducted in Ruijin Hospital, Shanghai Jiao Tong University; D.W. supervised studies in School of Life Sciences and Biotechnology, Shanghai Jiao Tong university; and Q.X. and W.W. designed experiments, analysed the data and wrote the manuscript. All authors approved the final version of this manuscript.

Funding

This study was supported by the National Natural Science Foundation of China (81570115, 31770772, 61832019 and 61503244), the Key Research Area Grant 2016YFA0501703 of the Ministry of Science and Technology of China, and Joint Research Funds for Translational Medicine at Shanghai Jiao Tong University (ZH2018ZDA06).

Conflict of Interest

None declared.

References

- Davie EW, Fujikawa K, Kisiel W. The coagulation cascade: initiation, maintenance, and regulation. *Biochemistry* 1991;30(43):10363–10370
- Uprichard J, Perry DJ. Factor X deficiency. *Blood Rev* 2002;16(02):97–110
- Menegatti M, Peyvandi F. Factor X deficiency. *Semin Thromb Hemost* 2009;35(04):407–415
- de Visser MC, Poort SR, Vos HL, Rosendaal FR, Bertina RM. Factor X levels, polymorphisms in the promoter region of factor X, and the risk of venous thrombosis. *Thromb Haemost* 2001;85(06):1011–1117
- Davie E, Ichinose A, Leytus S. Structural features of the proteins participating in blood coagulation and fibrinolysis. Cold Spring Harbor Symposia on Quantitative Biology. Cold Spring Harbor, NY: Cold Spring Harbor Laboratory Press; 1986:509–514
- Ding Q, Shen Y, Yang L, Wang X, Rezaie AR. The missense Thr211Pro mutation in the factor X activation peptide of a bleeding patient causes molecular defect in the clotting cascade. *Thromb Haemost* 2013;110(01):53–61
- Lu Q, Yang L, Manithody C, Wang X, Rezaie AR. Molecular basis of the clotting defect in a bleeding patient missing the Asp-185 codon in the factor X gene. *Thromb Res* 2014;134(05):1103–1109
- Roehrig S, Straub A, Pohlmann J, et al. Discovery of the novel antithrombotic agent 5-chloro-N-((5S)-2-oxo-3-[4-(3-oxomorpholin-4-yl)phenyl]-1,3-oxazolidin-5-ylmethyl)thiophene-2-carboxamide (BAY 59-7939): an oral, direct factor Xa inhibitor. *J Med Chem* 2005;48(19):5900–5908
- Pettersen EF, Goddard TD, Huang CC, et al. UCSF Chimera—a visualization system for exploratory research and analysis. *J Comput Chem* 2004;25(13):1605–1612
- Best RB, Zhu X, Shim J, et al. Optimization of the additive CHARMM all-atom protein force field targeting improved sampling of the backbone ϕ , ψ and side-chain $\chi(1)$ and $\chi(2)$ dihedral angles. *J Chem Theory Comput* 2012;8(09):3257–3273
- Abraham MJ, Murtola T, Schulz R, et al. GROMACS: high performance molecular simulations through multi-level parallelism from laptops to supercomputers. *SoftwareX* 2015;1–2:19–25
- Hess B. P-LINCS: a parallel linear constraint solver for molecular simulation. *J Chem Theory Comput* 2008;4(01):116–122
- Humphrey W, Dalke A, Schulten K. VMD: visual molecular dynamics. *J Mol Graphics* 1996;14(01):33–38, 27–28
- Doolittle RF. Step-by-step evolution of vertebrate blood coagulation. *Cold Spring Harb Symp Quant Biol* 2009;74:35–40
- Hedstrom L. Serine protease mechanism and specificity. *Chem Rev* 2002;102(12):4501–4524
- Messier T, Wong C, Bovill E, Long G, Church W. Factor X Stockton: a mild bleeding diathesis associated with an active site mutation in factor X. *Blood Coagulation Fibrinolysis* 1996;7(01):5–14
- Pinotti M, Camire RM, Baroni M, Rajab A, Marchetti G, Bernardi F. Impaired prothrombinase activity of factor X Gly381Asp results in severe familial CRM+ FX deficiency. *Thromb Haemost* 2003;89(02):243–248
- Abdel-Azeim S, Oliva R, Chermak E, De Cristofaro R, Cavallo L. Molecular dynamics characterization of five pathogenic factor X mutants associated with decreased catalytic activity. *Biochemistry* 2014;53(44):6992–7001
- Millar DS, Elliston L, Deex P, et al. Molecular analysis of the genotype-phenotype relationship in factor X deficiency. *Hum Genet* 2000;106(02):249–257
- Venkateswarlu D, Perera L, Darden T, Pedersen LG. Structure and dynamics of zymogen human blood coagulation factor X. *Biophys J* 2002;82(03):1190–1206
- Bode W, Schwager P, Huber R. The transition of bovine trypsinogen to a trypsin-like state upon strong ligand binding. The refined crystal structures of the bovine trypsinogen-pancreatic trypsin inhibitor complex and of its ternary complex with Ile-Val at 1.9 Å resolution. *J Mol Biol* 1978;118(01):99–112
- Toso R, Zhu H, Camire RM. The conformational switch from the factor X zymogen to protease state mediates exosite expression and prothrombinase assembly. *J Biol Chem* 2008;283(27):18627–18635
- Li W, Johnson DJ, Esmon CT, Huntington JA. Structure of the antithrombin-thrombin-heparin ternary complex reveals the antithrombotic mechanism of heparin. *Nat Struct Mol Biol* 2004;11(09):857–862
- Banner DW, D'Arcy A, Chène C, et al. The crystal structure of the complex of blood coagulation factor VIIa with soluble tissue factor. *Nature* 1996;380(6569):41–46
- Johnson DJ, Langdown J, Huntington JA. Molecular basis of factor IXa recognition by heparin-activated antithrombin revealed by a 1.7-Å structure of the ternary complex. *Proc Natl Acad Sci U S A* 2010;107(02):645–650
- Navaneetham D, Jin L, Pandey P, et al. Structural and mutational analyses of the molecular interactions between the catalytic domain of factor XIa and the Kunitz protease inhibitor domain of protease nexin 2. *J Biol Chem* 2005;280(43):36165–36175
- Girolami A, Scarparo P, Scandellari R, Allemand E. Congenital factor X deficiencies with a defect only or predominantly in the extrinsic or in the intrinsic system: a critical evaluation. *Am J Hematol* 2008;83(08):668–671
- Venkateswarlu D. Structural insights into the interaction of blood coagulation co-factor VIIIa with factor IXa: a computational protein-protein docking and molecular dynamics refinement study. *Biochem Biophys Res Commun* 2014;452(03):408–414
- Basu S, Biswas P. Salt-bridge dynamics in intrinsically disordered proteins: a trade-off between electrostatic interactions and structural flexibility. *Biochim Biophys Acta Proteins Proteomics* 2018;1866(5-6):624–641
- Lisgarten DR, Palmer RA, Lobley CMC, et al. Ultra-high resolution X-ray structures of two forms of human recombinant insulin at 100 K. *Chem Cent J* 2017;11(01):73
- Zhou A, Carrell RW, Murphy MP, et al. A redox switch in angiotensinogen modulates angiotensin release. *Nature* 2010;468(7320):108–111